ELECTRONIC RESEARCH ARCHIVE
Volume **29**, Number **3**, August **2021**

doi:10.3934/era.2020120
pp. **2375–2389**

A CONFORMING DISCONTINUOUS GALERKIN FINITE ELEMENT METHOD ON RECTANGULAR PARTITIONS

Yue Feng

Department of Mathematics, Jilin University
Changchun, China

Yujie Liu

Artificial Intelligence Research Center, Peng Cheng Laboratory
Shenzhen 518005, China

Ruishu Wang*

Department of Mathematics, Jilin University
Changchun, China

Shangyou Zhang

Department of Mathematical Sciences, University of Delaware
Newark, DE 19716, USA

Abstract. This article presents a conforming discontinuous Galerkin (conforming DG) scheme for second order elliptic equations on rectangular partitions. The new method is based on DG finite element space and uses a weak gradient arising from local Raviart Thomas space for gradient approximations. By using the weak gradient and enforcing inter-element continuity strongly, the scheme maintains the simple formulation of conforming finite element method while have the flexibility of using discontinuous approximations. Hence, the programming complexity of this new conforming DG scheme is significantly reduced compared to other existing DG methods. Error estimates of optimal order are established for the corresponding conforming DG approximations in various discrete Sobolev norms. Numerical results are presented to confirm the developed convergence theory.

2020 *Mathematics Subject Classification.* Primary: 65N15, 65N30; Secondary: 35B45, 35J50.

Key words and phrases. Conforming discontinuous Galerkin finite element method, second order elliptic problem, rectangular partitions, error estimates.

The research of the first author was supported in part by China Natural National Science Foundation (91630201, U1530116, 11726102, 11771179, 93K172018Z01, 11701210, JJKH20180113KJ, 20190103029JH), and by the Program for Cheung Kong Scholars of Ministry of Education of China, Key Laboratory of Symbolic Computation and Knowledge Engineering of Ministry of Education, Jilin University, Changchun 130012, China.

The research of Liu was partially supported by China Natural National Science Foundation (No. 12001306), Guangdong Provincial Natural Science Foundation (No. 2017A030310285).

The research of Wang was partially supported by China Natural National Science Foundation (No. 12001230), Postdoctoral Research Fund (No. 2019M661199, BX20190142).

* Corresponding author: Ruishu Wang.

1. **Introduction.** For simplicity, we consider Poisson equation with a Dirichlet boundary condition as our model problem.

$$-\Delta u = f, \text{ in } \Omega, \tag{1}$$

$$u = g, \text{ on } \partial\Omega, \tag{2}$$

where Ω is a bounded polygonal domain in $\mathbb{R}^2$.

Using integration by parts, we can get the variational form: find $u \in H^1(\Omega)$ satisfying $u = g$ on $\partial\Omega$ and

$$(\nabla u, \nabla v) = (f, v), \ \forall v \in H_0^1(\Omega). \tag{3}$$

Various finite element methods have been introduced to solve the Poisson equations (1)-(2), such as the Galerkin finite element methods (FEMs)[2, 3], the mixed FEMs [15] and the finite volume methods (FVMs) [6], etc. The FVMs emphasis on the local conservation property and discretize equations by asking the solution satisfying the flux conservation on a dual mesh consisting of control volumes. The mixed FEMs is another category method that based on the variable u and a flux variable usually written as p.

The classical conforming finite element method obtains numerical approximate results by constructing a finite-dimensional subspace of $H_0^1(\Omega)$. The finite element scheme has the same form with the variational form (3): find $u_h \in V_h \subset H^1(\Omega)$ satisfying $u_h = I_h g$ on $\partial\Omega$ and

$$(\nabla u_h, \nabla v_h) = (f, v_h), \ \forall v_h \in V_h^0, \tag{4}$$

where V_h^0 is a subspace of V_h that satisfying $v_h = 0$ on $\partial\Omega$ and I_h is the kth order Lagrange interpolation operator. The FE method is a popular and easy-to-implement numerical scheme, however, it is less flexible in constructing elements and generating meshes. These limitations are mainly due to the strong continuity requirements of functions in V_h. One solution to circumvent these limitations is using discontinuous approximations. Since the 1970th, many new finite element methods with discontinuous approximations have been developed, including the early proposed DG methods [1], local discontinuous Galerkin (LDG) methods [8], interior penalty discontinuous Galerkin (IPDG) methods [9], and the recently developed hybridizable discontinuous Galerkin (HDG) methods [7], mimetic finite differences method [10], virtual element (VE) method [4], weak Galerkin (WG) method [19, 20] and references therein.

One obvious disadvantage of discontinuous finite element methods is their rather complex formulations which are often necessary to ensure connections of discontinuous solutions across element boundaries. For example, the IPDG methods add parameter depending interior penalty terms. Besides additional programming complexity, one often has difficulties in finding optimal values for the penalty parameters and corresponding efficient solvers. Most recently, Zhang and Ye [21] developed a discontinuous finite element method that has an ultra simple weak formulation on triangular/tetrahedal meshes. The corresponding numerical scheme can be written as: find $u_h \in \tilde{V}_h$ satisfying $u_h = I_h g$ on $\partial\Omega$ and

$$(\nabla_w u_h, \nabla_w v_h) = (f, v_h), \ \forall v_h \in V_h^0, \tag{5}$$

where $\tilde{V}_h$ is the DG finite element space and ∇_w is the weak gradient operator. The notion of weak gradient was first introduced by Wang and Ye in the weak Galerkin (WG) methods [19, 20]. The WG methods allow the use of totally discontinuous functions and provides stable numerical schemes that are parameter-independent and free of locking [17] in some applications. Another key feature in the WG methods is it can be used for arbitrary polygonal meshes. The WG finite element method has been rapidly developed and applied to other problems, including the Stokes and Navier-Stokes equations [11, 18], the biharmonic [14, 13] and elasticity equations [12, 17], div-curl systems and the Maxwell's equations and parabolic problem [23], etc. The introduction of the weak gradient operator in the conforming DG methods makes the scheme (5) maintain the simple formulation of conforming finite element method while have the flexibility of using discontinuous approximations. Hence, the programming complexity of this conforming DG scheme is significantly reduced. Furthermore, the scheme results in a simple symmetric and positive definite system.

Following the work in [21, 22], we propose a new conforming DG finite element method on rectangular partitions in this work. It can be obtained from the conforming formulation simply by replacing ∇ by ∇_w and enforcing the boundary condition strongly. The simplicity of the conforming DG formulation will ease the complexity for implementation of DG methods. We note that the conforming DG method in [21] is based on triangular/tetrahedal meshes. Then in [22], the method is extended to work on general polytopal meshes by raising the degree of polynomials used to compute weak gradient.

In this paper, we keep the same finite element space as DG method, replace the boundary function with the average of the inner function, and use the weak gradient arising from local Raviart-Thomas (RT) elements [5] to approximate the classic gradient. Moreover, the derivation process in this paper is based on rectangular RT elements [16]. Error estimates of optimal order are established for the corresponding conforming DG approximation in both a discrete H^1 norm and the L^2 norm. Numerical verifications have been performed on different kinds of quadrangle finite element space. In particular, super-convergence phenomenon have been observed for Q_0 elements.

The rest of this paper is organized as follows: In Section 2, we shall present the conforming DG finite element scheme for the Poisson equation on rectangular partitions. Section 3 is devoted to a discussion of the stability and solvability of the new method. In Section 4, we shall prepare ourselves for error estimates by deriving some identities. Error estimates of optimal order in H^1 and L^2 norm are established in Section 5. In Section 6, we present some numerical results to illustrate the theory derived in earlier sections. Finally in section 7, we conclude our major contributions in this article.

Throughout this paper, we adopt the standard definition of Sobolev space $H^s(\Omega)$. For any given open bounded domain $K \subseteq \Omega$, $(\cdot,\cdot)_{s,K}$, $\|\cdot\|_{s,K}$, and $|\cdot|_{s,K}$ are used to denote the inner product, norm and semi-norm, respectively. The space $H^0(K)$ coincides with $L^2(K)$, and the subscripts K in the inner product, norm, and semi-norm can be dropped in the case of $K = \Omega$. In particular, the function space $H_0^1(\Omega)$ is defined as

$$H_0^1(\Omega) = \{v \in H^1(\Omega) : \ v|_{\partial\Omega} = 0\},$$

and the space $H(div, \Omega)$ is defined as the set of vector-valued functions $\boldsymbol{q}$, which together with their divergence are square integrable, i.e.

$$H(div, \Omega) = \{\boldsymbol{q} \in [L^2(\Omega)]^d : \ \nabla \cdot \boldsymbol{q} \in L^2(\Omega)\}.$$

2. **Conforming DG method.** Assume that the domain Ω is of polygonal type and is partitioned into non-overlapping rectangles $\mathcal{T}_h = \{T\}$. For each $T \in \mathcal{T}_h$,

denote by T^0 its interior and ∂T its boundary. Denote by $\mathcal{E}_h = \{e\}$ the set of all edges in $\mathcal{T}_h$, and $\mathcal{E}_h^0 = \mathcal{E}_h \backslash \partial\Omega$ the set of all interior edges in $\mathcal{T}_h$. For each $T \in \mathcal{T}_h$ and $e \in \mathcal{E}_h$, denote by h_T and h_e the diameter of T and e, respectively. $h = \max_{T\in\mathcal{T}_h} h_T$ is the meshsize of $\mathcal{T}_h$.

For any interior edge $e \in \mathcal{E}_h^0$, let T_1 and T_2 be two rectangles sharing e, we define the average $\{\cdot\}$ and the jump $[\![\cdot]\!]$ on e for a scalar-valued function v by

$$\{v\} \quad = \quad \frac{1}{2}(v|_{\partial T_1} + v|_{\partial T_2}),\ [\![v]\!] = v|_{\partial T_1}\boldsymbol{n}_1 + v|_{\partial T_2}\boldsymbol{n}_2, \tag{6}$$

where $v|_{\partial T_i}, i = 1, 2$ is the trace of v on ∂T_i, $\boldsymbol{n}_1$ and $\boldsymbol{n}_2$ are the two unit outward normal vectors on e, associated with T_1 and T_2, respectively. If e is a boundary edge, we define

$$\{v\} \quad = \quad v|_e \text{ and } [\![v]\!] = v|_e\boldsymbol{n}. \tag{7}$$

We define a discontinuous finite element space

$$V_h = \{v \in L^2(\Omega) : v|_T \in Q_k(T),\ \forall\ T \in \mathcal{T}_h\}, \tag{8}$$

and its subspace

$$V_h^0 = \{v \in V_h : v = 0 \text{ on } \partial\Omega\}, \tag{9}$$

where $Q_k(T),\ k \geq 1$ denotes the set of polynomials with regard to quadrilateral elements. The weak gradient for a scalar-valued function $v \in V_h$ is defined by the following definition

Definition 2.1. For a given $T \in \mathcal{T}_h$ and a function $v \in V_h$, the discrete weak gradient $\nabla_d v \in RT_k(T)$ on T is defined as the unique polynomial such that

$$(\nabla_d v, \boldsymbol{q})_T := -(v, \nabla\cdot\boldsymbol{q})_T + \langle\{v\}, \boldsymbol{q}\cdot\boldsymbol{n}\rangle_{\partial T},\ \forall\ \boldsymbol{q} \in RT_k(T), \tag{10}$$

where $\boldsymbol{n}$ is the unit outward normal on ∂T, $RT_k(T) = [Q_k(T)]^2 + \mathbf{x}Q_k(T)$, and $\{v\}$ is defined in (6) and (7).

The weak gradient operator ∇_d as defined in (10) is a local operator computed at each element. It can be extended to any function $v \in V_h$ by taking weak gradient locally on each element T. More precisely, the weak gradient of any $v \in V_h$ is defined element-by-element as follows:

$$(\nabla_d v)|_T = \nabla_d(v|_T).$$

We introduce the following bilinear form:

$$a(v, w) = (\nabla_d v, \nabla_d w),$$

the conforming DG algorithm to solve the problems (1) - (2) is given by

Conforming DG algorithm 1. *Find $u_h \in V_h$ satisfying $u_h = I_h g$ on $\partial\Omega$ and*

$$a(u_h, v_h) = (f, v_h),\ \forall\ v_h \in V_h^0, \tag{11}$$

where I_h is the kth order Lagrange interpolation.

3. Stability and well-posedness.

We will prove the existence and uniqueness of the solution of equation (11). Firstly, we present the following two useful inequalities to derive the forthcoming analysis.

Lemma 3.1 (trace inequality)**.** *Let T be an element of the finite element partition $\mathcal{T}_h$, and e is an edge or face which is part of ∂T. For any function $\varphi \in H^1(T)$, the following trace inequality holds true (see [20] for details):*

$$\|\varphi\|_e^2 \le C(h_T^{-1}\|\varphi\|_T^2 + h_T\|\nabla\varphi\|_T^2), \tag{12}$$

where C is a constant independent of h.

Lemma 3.2 (inverse inequality)**.** *Let $\mathcal{T}_h$ be a finite element partition of Ω that is shape regualr. Assume that $\mathcal{T}_h$ satisfies all the assumptions A1-A4 in [20]. Then, for any piecewise polynomial function φ of degree n on $\mathcal{T}_h$, there exists a constant $C = C(n)$ such that*

$$\|\nabla\varphi\|_T \le C(n)h_T^{-1}\|\varphi\|_T, \ \forall T \in \mathcal{T}_h. \tag{13}$$

Then, we define the following semi-norms in the discontinuous finite element space V_h

$$|\!|\!| v |\!|\!|^2 = a(v,v) = \sum_{T\in\mathcal{T}_h} \|\nabla_d v\|_T^2, \tag{14}$$

$$\|v\|_{1,h}^2 = \sum_{T\in\mathcal{T}_h} \|\nabla v\|_T^2 + \sum_{e\in\mathcal{E}_h^0} h_e^{-1}\|[\![v]\!]\|_e^2. \tag{15}$$

We have the equivalence between the semi-norms $|\!|\!| v |\!|\!|$ and $\|v\|_{1,h}$, and it is proved in the following lemma.

Lemma 3.3. *For any $v \in V_h$, the following equivalence holds true*

$$C_1\|v\|_{1,h} \le |\!|\!| v |\!|\!| \le C_2\|v\|_{1,h}, \tag{16}$$

where C_1 and C_2 are two constants independent of h.

Proof. It follows from the definition of $\nabla_d v$, integration by parts, the trace inequality, and the inverse inequality that

$$\begin{aligned}
\|\nabla_d v\|_{T_1}^2 &= (\nabla_d v, \nabla_d v)_{T_1} = -(v, \nabla\cdot\nabla_d v)_{T_1} + \langle\{v\}\boldsymbol{n}, \nabla_d v\rangle_{\partial T_1} \\
&= (\nabla v, \nabla_d v)_{T_1} - \langle(v-\{v\})\boldsymbol{n}, \nabla_d v\rangle_{\partial T_1} \\
&\le \|\nabla v\|_{T_1}\|\nabla_d v\|_{T_1} + \|(v-\{v\})\boldsymbol{n}\|_{\partial T_1}\|\nabla_d v\|_{\partial T_1} \\
&\le \|\nabla_d v\|_{T_1}(\|\nabla v\|_{T_1} + h_{T_1}^{-\frac{1}{2}}\|(v-\{v\})\boldsymbol{n}\|_{\partial T_1}).
\end{aligned} \tag{17}$$

For any $e \subset \partial T_1$, $e = \partial T_1 \cap \partial T_2$, we have

$$\begin{aligned}
(v-\{v\})|_e\boldsymbol{n}_1 &= v|_{\partial T_1}\boldsymbol{n}_1 - \frac{1}{2}(v|_{\partial T_1} + v|_{\partial T_2})\boldsymbol{n}_1 \\
&= \frac{1}{2}(v|_{\partial T_1}\boldsymbol{n}_1 + v|_{\partial T_2}\boldsymbol{n}_2) \\
&= \frac{1}{2}[\![v]\!]_e.
\end{aligned}$$

Then we can get

$$\|(v-\{v\})\boldsymbol{n}\|_{\partial T_1}^2 \le \frac{1}{2}\sum_{e\in\partial T_1}\|[\![v]\!]\|_e^2. \tag{18}$$

Substituting (18) into (17) gives

$$\|\nabla_d v\|_{T_1}^2 \quad \leq \quad C_2\|\nabla_d v\|_{T_1}(\|\nabla v\|_{T_1} + \sum_{e\in\partial T_1} h_e^{-\frac{1}{2}}\|[\![v]\!]\|_e),$$

this completes the proof of the right-hand of (16).

To prove the left-hand of (16), we consider the subspace of $RT_k(T)$ for any $T \in \mathcal{T}_h$

$$D(k,T) := \{\mathbf{q} \in RT_k(T) : \ \boldsymbol{q}\cdot\boldsymbol{n} = 0 \text{ on } \partial T\}.$$

Note that $D(k,T)$ is a dual space of $[Q_{k-1}(T)]^2$ [13]. Thus, for any $\nabla v \in [Q_{k-1}(T)]^2$, we have

$$\|\nabla v\|_T = \sup_{\boldsymbol{q}\in D(k,T)} \frac{(\nabla v, \boldsymbol{q})_T}{\|\boldsymbol{q}\|_T}. \tag{19}$$

Using the integration by parts, Cauchy-Schwarz inequality, the definition of $D(k,T)$ and $\nabla_d v$, we get

$$\begin{aligned}(\nabla v, \boldsymbol{q})_T &= -(v, \nabla\cdot\boldsymbol{q})_T + \langle v, \boldsymbol{q}\cdot\boldsymbol{n}\rangle_{\partial T}\\ &= (\nabla_d v, \boldsymbol{q})_T - \langle \{v\}, \boldsymbol{q}\cdot\boldsymbol{n}\rangle_{\partial T}\\ &= (\nabla_d v, \boldsymbol{q})_T\\ &\leq \|\nabla_d v\|_T \cdot \|\boldsymbol{q}\|_T,\end{aligned}$$

where we have used the fact that $\boldsymbol{q}\cdot\boldsymbol{n}|_{\partial T} = 0$ in the definition of $D(k,T)$. Combining the above result with (19), one has

$$\|\nabla v\|_T \leq \|\nabla_d v\|_T. \tag{20}$$

We define the space $D_e(k,T)$ as the set of all $\boldsymbol{q} \in RT_k(T)$ such that all degrees of freedom, except those for $\boldsymbol{q}\cdot\boldsymbol{n}|_e$, vanish. Note that $D_e(k,T)$ is a dual space of $[Q_k(e)]^2$ [13]. Thus, we know

$$\|[\![v]\!]\|_e = \sup_{\boldsymbol{q}\in D_e(k,T)} \frac{\langle [\![v]\!], \boldsymbol{q}\cdot\boldsymbol{n}\rangle_e}{\|\boldsymbol{q}\cdot\boldsymbol{n}\|_e}. \tag{21}$$

Following the integration by parts and the definition of ∇_d, we can derive that

$$(\nabla_d v, \boldsymbol{q})_T = (\nabla v, \boldsymbol{q})_T - \langle v, \boldsymbol{q}\cdot\boldsymbol{n}\rangle_e + \langle \{v\}, \boldsymbol{q}\cdot\boldsymbol{n}\rangle_e.$$

Together with (20), we obtain

$$\begin{aligned}|\langle [\![v]\!], \boldsymbol{q}\cdot\boldsymbol{n}\rangle_e| &= 2|(\nabla_d v, \boldsymbol{q})_T - (\nabla v, \boldsymbol{q})_T|\\ &\leq 2|(\nabla_d v, \boldsymbol{q})_T| + 2|(\nabla v, \boldsymbol{q})_T|\\ &\leq C(\|\nabla_d v\|_T\|\boldsymbol{q}\|_T + \|\nabla v\|_T\|\boldsymbol{q}\|_T)\\ &\leq C\|\nabla_d v\|_T\|\boldsymbol{q}\|_T.\end{aligned}$$

Substituting the above inequality into (21), by the scaling argument [13], for such $\boldsymbol{q} \in D_e(k,T)$, we have $\|\boldsymbol{q}\|_T \leq h^{\frac{1}{2}}\|\boldsymbol{q}\cdot\boldsymbol{n}\|_e$, then

$$\|[\![v]\!]\|_e \leq C\frac{\|\nabla_d v\|_T\|\boldsymbol{q}\|_T}{\|\boldsymbol{q}\cdot\boldsymbol{n}\|_e} \leq Ch^{\frac{1}{2}}\|\nabla_d v\|_T. \tag{22}$$

Combining (20) and (22) gives a proof of the left-hand of (16). □

Lemma 3.4. *The semi-norm* $|\!|\!|\cdot|\!|\!|$ *defined in (14) is a norm in* V_h^0.

Proof. We shall only verify the positivity property for $|\!|\!|\cdot|\!|\!|$. To this end, assume $|\!|\!|v|\!|\!| = 0$ for some $v \in V_h^0$. By Lemma 3.3, it follows that $\|v\|_{1,h} = 0$ for all $T \in \mathcal{T}_h$, which means that $\nabla v = \boldsymbol{0}$ for all elements $T \in \mathcal{T}_h$ and $[\![v]\!] = 0$ for all edges $e \in \mathcal{E}_h^0$. We can derive from $\nabla v = \boldsymbol{0}$ for all $T \in \mathcal{T}_h$ that v is a constant in each T. $[\![v]\!] = 0$ on each $e \in \mathcal{E}_h^0$ implies v is a continuous function. This two conclusions and $v = 0$ on $\partial\Omega$ show that $v = 0$, which completes the proof of the lemma. □

The above two lemmas imply the well posedness of the scheme (11). We prove the existence and uniqueness of solution of the conforming DG method in Theorem 3.1.

Theorem 3.1. *The conforming DG scheme (11) has and only has one solution.*

Proof. To prove the scheme (11) is uniquely solvable, it suffices to verify that the homogeneous equation has zero as its unique solution. To this end, let $u_h \in V_h$ be the solution of the numerical scheme 11 with homogeneous data $f = 0$, $g = 0$. Letting $v_h = u_h$, we obtain

$$a(u_h, u_h) = 0,$$

which leads to $u_h = 0$ by using Lemma 3.4. This completes the proof of the theorem. □

4. **Error equation.** In this section, we will derive an error equation which will be used for the error estimates. For any $\boldsymbol{q} \in H(div, \Omega)$, we assume that there exist an interpolation operator Π_h satisfying $\Pi_h \boldsymbol{q} \in H(div, \Omega) \cap RT_k(T)$ on each element $T \in \mathcal{T}_h$ and

$$(\nabla \cdot \boldsymbol{q}, v)_T = (\nabla \cdot \Pi_h \boldsymbol{q}, v)_T, \ \forall v \in Q_k(T). \tag{23}$$

For any $w \in H^{1+k}(\Omega)$ with $k \geq 1$, from Lemma 7.3 in [20], we have the estimate of Π_h as follows.

$$\|\Pi_h(\nabla w) - \nabla w\| \leq Ch^k \|w\|_{1+k}. \tag{24}$$

Moreover, it is easy to verify the following property holds true.

Lemma 4.1. *For any $\boldsymbol{q} \in H(div, \Omega)$,*

$$\sum_{T\in\mathcal{T}_h} (-\nabla \cdot \boldsymbol{q}, v)_T = \sum_{T\in\mathcal{T}_h} (\Pi_h \boldsymbol{q}, \nabla_d v)_T, \ \forall v \in V_h^0. \tag{25}$$

Proof. $\Pi_h \boldsymbol{q} \in H(div, \Omega)$ implies that $\Pi_h \boldsymbol{q}$ is continuous across each interior edge. Since $v \in V_h^0$, we know that $\{v\} = v = 0$ on $\partial\Omega$. Then

$$\sum_{T\in\mathcal{T}_h} \langle \{v\}, \Pi_h \boldsymbol{q} \cdot \boldsymbol{n} \rangle_{\partial T} = 0. \tag{26}$$

By the definition of Π_h and ∇_d and the equation (26), we have

$$\begin{aligned}
\sum_{T\in\mathcal{T}_h} (-\nabla \cdot \boldsymbol{q}, v)_T &= \sum_{T\in\mathcal{T}_h} (-\nabla \cdot \Pi_h \boldsymbol{q}, v)_T \\
&= \sum_{T\in\mathcal{T}_h} (-\nabla \cdot \Pi_h \boldsymbol{q}, v)_T + \sum_{T\in\mathcal{T}_h} \langle \{v\}, \Pi_h \boldsymbol{q} \cdot \boldsymbol{n} \rangle_{\partial T} \\
&= \sum_{T\in\mathcal{T}_h} (\Pi_h \boldsymbol{q}, \nabla_d v)_T.
\end{aligned}$$

This completes the proof of the lemma. □

Before establishing the error equation, we define a continuous finite element subspace of V_h as follows

$$\tilde{V}_h = \{v \in H^1(\Omega) : v|_T \in Q_k(T),\ \forall T \in \mathcal{T}_h\}. \tag{27}$$

so as a subspace of $\tilde{V}_h$

$$\tilde{V}_h^0 := \{v \in \tilde{V}_h : v|_{\partial\Omega} = 0\}. \tag{28}$$

Lemma 4.2. *For any $v \in \tilde{V}_h$, we have*

$$\nabla_d v = \nabla v.$$

Proof. By the definition of ∇_d and integration by parts, for any $\boldsymbol{q} \in RT_k(T)$, we have

$$\begin{aligned}
(\nabla_d v, \boldsymbol{q})_T &= -(v, \nabla \cdot \boldsymbol{q})_T + \langle \{v\}, \boldsymbol{q} \cdot \boldsymbol{n} \rangle_{\partial T} \\
&= -(v, \nabla \cdot \boldsymbol{q})_T + \langle v, \boldsymbol{q} \cdot \boldsymbol{n} \rangle_{\partial T} \\
&= (\nabla v, \boldsymbol{q})_T,
\end{aligned}$$

which gives

$$(\nabla_d v - \nabla v, \boldsymbol{q})_T = 0,\ \forall \boldsymbol{q} \in RT_k(T).$$

Letting $\boldsymbol{q}$ be $\nabla_d v - \nabla v$ in the above equation yields $\|\nabla_d v - \nabla v\| = 0$, which completes the proof of the lemma. □

Let $e_h = I_h u - u_h$, where I_h is the kth order Lagrange interpolation, $u \in H^{k+1}(\Omega)$ with $k \geq 1$ is the exact solution of the Poisson equations (1) - (2), and $u_h \in V_h$ is the numerical solution of the scheme (11). The following estimate of the Lagrange interpolation operator I_h holds true.

$$\|I_h u - u\| \leq C h^{k+1} \|u\|_{k+1}, \tag{29}$$

$$\|\nabla I_h u - \nabla u\| \leq C h^k \|u\|_{k+1}. \tag{30}$$

It is obvious that $e_h \in V_h^0$ and $I_h u \in \tilde{V}_h$. We have the following lemma:

Lemma 4.3. *Denote $e_h = I_h u - u_h$ the error of conforming DG method arising from (11). For any $v_h \in V_h^0$, we have*

$$a(e_h, v_h) = l_u(v_h), \tag{31}$$

where

$$l_u(v_h) = \sum_{T \in \mathcal{T}_h} (\nabla I_h u - \Pi_h \nabla u, \nabla_d v_h). \tag{32}$$

Proof. Since $I_h u \in \tilde{V}_h$, we have $\nabla_d I_h u = \nabla I_h u$. Using the property (25), we can derive

$$\begin{aligned}
\sum_{T \in \mathcal{T}_h} (\nabla_d I_h u, \nabla_d v_h)_T &= \sum_{T \in \mathcal{T}_h} (\nabla I_h u, \nabla_d v_h)_T \\
&= \sum_{T \in \mathcal{T}_h} (\nabla I_h u - \Pi_h \nabla u + \Pi_h \nabla u, \nabla_d v_h)_T \\
&= \sum_{T \in \mathcal{T}_h} (\nabla I_h u - \Pi_h \nabla u, \nabla_d v_h)_T + \sum_{T \in \mathcal{T}_h} (\Pi_h \nabla u, \nabla_d v_h)_T \\
&= l_u(v_h) - \sum_{T \in \mathcal{T}_h} (\nabla \cdot \nabla u, v_h)_T \\
&= l_u(v_h) + (f, v_h).
\end{aligned}$$

By the definition of the scheme (11), we have

$$\sum_{T\in\mathcal{T}_h}(\nabla_d I_h u-\nabla_d u_h,\nabla_d v_h)_T=l_u(v_h).$$

This completes the proof of the lemma. □

5. **Error estimates.** The goal of this section is to derive the error estimates in H^1 and L^2 norms for the conforming DG solution u_h.

Theorem 5.1. *Let $u\in H^{k+1}(\Omega)$ with $k\geq 1$ be the exact solution of the Poisson equation (1) - (2), and $u_h\in V_h$ be the numerical solution of the scheme (11). Let $e_h=I_hu-u_h$, there exists a constant C independent of h such that*

$$|||e_h|||\leq Ch^k|u|_{k+1}. \tag{33}$$

Proof. Letting $v_h=e_h$ in (31), and by the definition of $|||\cdot|||$, we have

$$|||e_h|||^2=l_u(e_h). \tag{34}$$

From the Cauchy-Schwarz inequality, the triangle inequality, the definition of $|||\cdot|||$, (24), and (30), we arrive at

$$\begin{aligned}
l_u(v_h) &= \sum_{T\in\mathcal{T}_h}(\nabla I_h u-\Pi_h(\nabla u),\nabla_d v_h)_T\\
&\leq \sum_{T\in\mathcal{T}_h}\|\nabla I_h u-\Pi_h(\nabla u)\|_T\|\nabla_d v_h\|_T\\
&\leq \left(\sum_{T\in\mathcal{T}_h}\|\nabla I_h u-\Pi_h(\nabla u)\|_T^2\right)^{\frac12}\left(\sum_{T\in\mathcal{T}_h}\|\nabla_d v_h\|_T^2\right)^{\frac12}\\
&= \left(\sum_{T\in\mathcal{T}_h}\|\nabla I_h u-\nabla u+\nabla u-\Pi_h(\nabla u)\|_T^2\right)^{\frac12}|||v_h|||\\
&\leq \left(\sum_{T\in\mathcal{T}_h}\|\nabla I_h u-\nabla u\|_T^2+\|\nabla u-\Pi_h(\nabla u)\|_T^2\right)^{\frac12}|||v_h|||\\
&\leq Ch^k|u|_{k+1}|||v_h|||.
\end{aligned}$$

Then, we have

$$l_u(e_h)\leq Ch^k|u|_{k+1}|||e_h|||. \tag{35}$$

Substituting (35) to (34), we obtain

$$|||e_h|||^2\leq Ch^k|u|_{k+1}|||e_h|||,$$

which completes the proof of the lemma. □

It is obvious that $\tilde{V}_h^0\subset V_h^0$. Let $\tilde{u}_h\in\tilde{V}_h$ be the finite element solution for the problem (1)-(2) which satisfies $\tilde{u}_h=I_hg$ on $\partial\Omega$ and

$$(\nabla\tilde{u}_h,\nabla v)=(f,v),\ \forall v\in\tilde{V}_h^0. \tag{36}$$

For any $v\in\tilde{V}_h^0\subset\tilde{V}_h$, we have $\nabla_d v=\nabla v$, i.e.

$$(\nabla_d u_h-\nabla\tilde{u}_h,\nabla v)=0,\ \forall v\in\tilde{V}_h^0. \tag{37}$$

In the rest of this section, we derive an optimal order error estimate for the conforming DG approximation (11) in L^2 norm by adopting the duality argument. To this end, we consider the following dual problem that seeks $\Phi \in H_0^1(\Omega)$ satisfying

$$-\nabla \cdot (\nabla \Phi) = u_h - \tilde{u}_h, \ \textit{in } \Omega. \tag{38}$$

Assume that the dual problem satisfies H^2-regularity, which means the following priori estimate holds true

$$\|\Phi\|_2 \leq C\|u_h - \tilde{u}_h\|. \tag{39}$$

In the following of this paper, we note $\varepsilon_h = u_h - \tilde{u}_h$ for simplicity.

Theorem 5.2. *Assume $u \in H^{k+1}(\Omega)$ with $k \geq 1$ is the exact solution of the Poisson equation (1) - (2), and $u_h \in V_h$ is the numerical solution obtained with the scheme (11). Furthermore, assume that (39) holds true. Then, there exists a constant C independent of h such that*

$$\|u - u_h\| \leq Ch^{k+1}|u|_{k+1}. \tag{40}$$

Proof. First, we shall derive the optimal order for ε_h in L^2 norm. Consider the corresponding conforming DG scheme defined in (11) and let $\Phi_h \in V_h^0$ be the solution satisfying

$$a(\Phi_h, v) = (\varepsilon_h, v), \ \forall v \in V_h^0. \tag{41}$$

Since $I_h\Phi \in \tilde{V}_h$, it follows from (37) that

$$\begin{aligned} (\nabla_d u_h - \nabla \tilde{u}_h, \nabla I_h \Phi) &= 0, \\ \nabla_d I_h \Phi &= \nabla I_h \Phi, \end{aligned}$$

which gives

$$(\nabla_d u_h - \nabla \tilde{u}_h, \nabla_d I_h \Phi) = 0. \tag{42}$$

Setting $v = \varepsilon_h$ in (41), then by the definition of ε_h and (42), we have

$$\begin{aligned} \|\varepsilon_h\|^2 &= a(\Phi_h, \varepsilon_h) = \sum_{T \in \mathcal{T}_h} (\nabla_d \Phi_h, \nabla_d \varepsilon_h)_T \\ &= \sum_{T \in \mathcal{T}_h} (\nabla_d(\Phi_h - I_h\Phi), \nabla_d u_h - \nabla \tilde{u}_h)_T \\ &\leq \|\!|\Phi_h - I_h\Phi|\!\|(\|\!|u_h - I_h u|\!\| + \|\nabla(I_h u - \tilde{u}_h)\|). \end{aligned}$$

Then, by the Cauchy-Schwarz inequality, (33) and (39), we obtain

$$\|\varepsilon_h\|^2 \leq Ch|\Phi|_2 h^k |u|_{k+1} \leq Ch^{k+1}|u|_{k+1}\|\varepsilon_h\|,$$

which gives

$$\|\varepsilon_h\| \leq Ch^{k+1}|u|_{k+1}. \tag{43}$$

Combining the error estimate of finite element solution, the triangle inequality and (43) yields (40), which completes the proof of the theorem. □

6. **Numerical experiments.** In this section, we shall present some numerical results for the conforming discontinuous Galerkin method analyzed in the previous sections.

We solve the following Poisson equation on the unit square domain $\Omega = (0,1) \times (0,1)$,

$$-\Delta u = 2\pi^2 \sin(\pi x)\sin(\pi y) \qquad \text{in } \Omega \tag{44}$$

$$u = 0 \qquad \text{on } \partial\Omega. \tag{45}$$

The exact solution of the above problem is $u = \sin(\pi x)\sin(\pi y)$. Uniform square grids as shown in Figure 1 are used for computation.

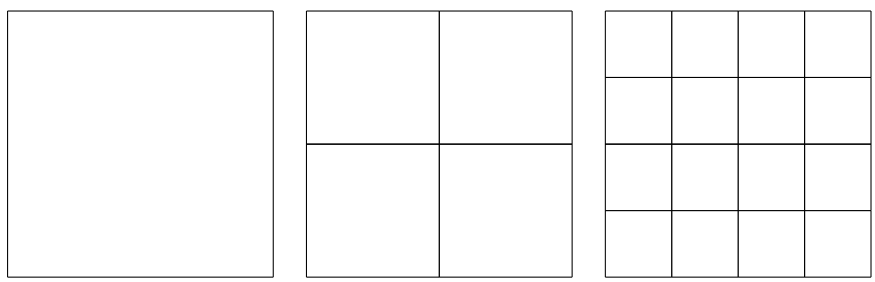

FIGURE 1. The first three grids used in the computation.

We first use the P_k conforming discontinuous Galerkin spaces (8) to compute the test case (44)-(45), where P_k denotes the set of polynomials of 2 variables of degree less than or equal to k. The weak gradient is computed locally using rectangular RT_k polynomials. The errors and the order of convergence of the conforming DG approximations are listed in Table 1. Optimal order of convergence is achieved in every case, which is consistent with our theory. In particular, a superconvergence of order $\mathcal{O}(h^2)$ was observed in the discrete H^1 norm for P_0 elements. Furthermore, the results obtained with P_0 elements seems to be slightly better than that obtained with P_1 elements.

The same test case is also computed using the Q_k conforming DG finite element space, where Q_k denotes the set of polynomials of 2 variables defined on Ω, and for each variable, the degree of the variable is at most k. Table 2 illustrates the numerical performance of the corresponding conforming DG scheme. It can be seen from numerical computing that, in this case, the results obtained with the Q_1 element are more accurate than those obtained with $Q_0(= P_0)$ elements (see Table 1). All numerical results converge at the corresponding optimal order, which is consistent with the theory.

To test the superconvergence of P_0 DG element, we solve the following 2nd order elliptic equation on the unit square domain $\Omega = (0,1) \times (0,1)$,

$$-\Delta u + u = f \qquad \text{in } \Omega$$

$$u = 0 \qquad \text{on } \partial\Omega,$$

where f is chosen so that the exact solution is not symmetric,

$$u = (x - x^2)(y - y^3). \tag{46}$$

TABLE 1. Error profiles and convergence rates for test case (44)-(45) obtained with uniform grids and P_k conforming DG spaces.

level	$\|u_h - Q_h u\|_0$	rate	$\|\|\|u_h - Q_h u\|\|\|$	rate	$\#Dof$
	by P_0 conforming discontinuous Galerkin elements				
6	0.1996E-02	1.97	0.8887E-02	1.98	1024
7	0.5013E-03	1.99	0.2228E-02	2.00	4096
8	0.1255E-03	2.00	0.5574E-03	2.00	16384
	by P_1 conforming discontinuous Galerkin elements				
6	0.2427E-02	1.97	0.1027E+00	1.02	3072
7	0.6100E-03	1.99	0.5105E-01	1.01	12288
8	0.1527E-03	2.00	0.2546E-01	1.00	49152
	by P_2 conforming discontinuous Galerkin elements				
5	0.1533E-03	3.00	0.2042E-01	2.03	1536
6	0.1915E-04	3.00	0.5061E-02	2.01	6144
7	0.2394E-05	3.00	0.1260E-02	2.01	24576
	by P_3 conforming discontinuous Galerkin elements				
5	0.7959E-05	4.00	0.1965E-02	3.00	2560
6	0.4971E-06	4.00	0.2451E-03	3.00	10240
7	0.3140E-07	3.98	0.3059E-04	3.00	40960
	by P_4 conforming discontinuous Galerkin elements				
4	0.1055E-04	4.97	0.1421E-02	4.05	960
5	0.3314E-06	4.99	0.8735E-04	4.02	3840
6	0.1057E-07	4.97	0.5417E-05	4.01	15360
	by P_5 conforming discontinuous Galerkin elements				
2	0.2835E-02	6.24	0.1450E+00	5.49	84
3	0.4532E-04	5.97	0.4718E-02	4.94	336
4	0.7115E-06	5.99	0.1478E-03	5.00	1344

Uniform square grids as shown in Figure 1 are used for numerical computation. The numerical results are listed in Table 3. Surprising, for this problem, the H^1-like norm of error superconverges at 1.5 order, and the L^2 error has one order of superconvergence. But we do not yet know if such a superconvergence exists in general.

To test further the superconvergence of P_0 DG element, we solve the following 2nd order elliptic equations on the unit square domain $\Omega = (0,1) \times (0,1)$,

$$\begin{aligned} -\nabla(a\nabla u) &= f && \text{in } \Omega \\ u &= 0 && \text{on } \partial\Omega, \end{aligned}$$

where $a = 1 + x + y$ and f is chosen so that the exact solution is not symmetric,

$$u = (x - x^3)(y^2 - y^3). \tag{47}$$

TABLE 2. Error profiles and convergence rates for test case (44)-(45) obtained with uniform grids and Q_k conforming DG spaces.

level	$\|u_h - Q_h u\|_0$	rate	$\|\|\|u_h - Q_h u\|\|\|$	rate	$\#Dof$
	by Q_1 conforming discontinuous Galerkin elements				
6	0.4006E-03	1.99	0.2389E-02	1.99	4096
7	0.1003E-03	2.00	0.5982E-03	2.00	16384
8	0.2510E-04	2.00	0.1496E-03	2.00	65536
	by Q_2 conforming discontinuous Galerkin elements				
6	0.2360E-04	2.99	0.3186E-02	1.99	9216
7	0.2953E-05	3.00	0.7976E-03	2.00	36864
8	0.3692E-06	3.00	0.1995E-03	2.00	147456
	by Q_3 conforming discontinuous Galerkin elements				
5	0.1413E-04	4.08	0.1650E-02	2.97	4096
6	0.8676E-06	4.03	0.2072E-03	2.99	16384
7	0.5398E-07	4.01	0.2593E-04	3.00	65536
	by Q_4 conforming discontinuous Galerkin elements				
3	0.2226E-02	4.59	0.5414E-01	3.52	400
4	0.9610E-04	4.53	0.3723E-02	3.86	1600
5	0.3279E-05	4.87	0.2392E-03	3.96	6400

TABLE 3. Error profiles and convergence rates for test case (46) obtained with uniform grids and P_0 conforming DG spaces.

level	$\|u_h - Q_h u\|_0$	rate	$\|\|\|u_h - Q_h u\|\|\|$	rate	$\#Dof$
	by P_0 conforming discontinuous Galerkin elements				
3	0.8265E-02	1.06	0.4577E-01	1.14	16
4	0.2772E-02	1.58	0.1732E-01	1.40	64
5	0.7965E-03	1.80	0.6331E-02	1.45	256
6	0.2142E-03	1.90	0.2290E-02	1.47	1024
7	0.5564E-04	1.94	0.8213E-03	1.48	4096
8	0.1419E-04	1.97	0.2928E-03	1.49	16384

Uniform square grids as shown in Figure 1 are used for computation. The numerical results are listed in Table 4. Surprising, again, the H^1-like norm of error superconverges at 1.5 order, and the L^2 error has one order of superconvergence for this problem.

7. **Conclusion.** In this paper, we establish a new numerical approximation scheme based on the rectangular partition to solve second order elliptic equation. We derived the numerical scheme and then proved the optimal order of convergence of the error estimates in L^2 and H^1 norms of the conforming DG method. Numerical experiments are then present to verify the theoretical analysis, and all numerical results converging at the corresponding optimal order. Comparing with existing numerical methods, the confoming DG method has the following two characteristics:
1. The formulation is relatively simple. The stabilizer $s(\cdot\ ,\ \cdot)$ is no longer needed,

TABLE 4. Error profiles and convergence rates for test case (47) obtained with uniform grids and P_0 conforming DG spaces.

level	$\|u_h - Q_h u\|_0$	rate	$\|\|u_h - Q_h u\|\|$	rate	$\#Dof$
	by P_0 conforming discontinuous Galerkin elements				
3	0.4929E-02	0.97	0.5371E-01	0.80	16
4	0.1917E-02	1.36	0.2401E-01	1.16	64
5	0.6004E-03	1.67	0.9407E-02	1.35	256
6	0.1682E-03	1.84	0.3507E-02	1.42	1024
7	0.4457E-04	1.92	0.1275E-02	1.46	4096
8	0.1148E-04	1.96	0.4576E-03	1.48	16384

and the boundary function u_b is omitted, which is replaced by the average of internal function u_0; 2. The projection operator Q_h used in the traditional WG method is replaced by the Lagrange interpolation operator I_h, which makes the theoretical analysis much easier. As can be seen from the numerical examples in Section 6, this method reduces the programming complexity while ensuring the optimal order of convergence.

REFERENCES

[1] D. N. Arnold, F. Brezzi, B. Cockburn and L. D. Marini, Unified analysis of discontinuous Galerkin methods for elliptic problems, *SIAM J. Numer. Anal.*, **39** (2001/02), 1749–1779.

[2] I. Babuška, The finite element method with penalty, *Math. Comp.*, **27** (1973), 221–228.

[3] G. A. Baker, Finite element methods for elliptic equations using nonconforming elements, *Math. Comp.*, **31** (1977), 45–59.

[4] L. Beirão da Veiga, F. Brezzi, A. Cangiani, G. Manzini, L. D. Marini and A. Russo, Basic principles of virtual element methods, *Math. Models Methods Appl. Sci.*, **23** (2013), 199–214.

[5] F. Brezzi, On the existence, uniqueness, and approximation of saddle point problems arising from Lagrangian multipliers, *RAIRO*, **8** (1974), 129–151.

[6] P. Chatzipantelidis, A finite volume method based on the Crouzeix-Raviart element for elliptic PDE's in two dimensions, *Numer. Math.*, **82** (1999), 409–432.

[7] G. Chen, W. Hu, J. Shen, J. R. Singler, Y. Zhang and X. Zheng, An HDG method for distributed control of convection diffusion PDEs, *J. Comput. Appl. Math.*, **343** (2018), 643–661.

[8] X. Feng and T. Lewis, Local discontinuous Galerkin methods for one-dimensional second order fully nonlinear elliptic and parabolic equations, *J. Sci. Comput.*, **59** (2014), 129–157.

[9] X. Feng, M. Neilan and S. Schenake, Interior penalty discontinuous Galerkin methods for second order linear non-divergence form elliptic PDEs, *J. Sci. Comput.*, **74** (2018), 1651–1676.

[10] K. Lipnikov, G. Manzini, F. Brezzi and A. Buffa, The mimetic finite difference method for the 3D magnetostatic field problems on polyhedral meshes, *J. Comput. Phys.*, **230** (2011), 305–328.

[11] Y. Liu and J. Wang, Simplified weak Galerkin and new finite difference schemes for the Stokes equation, *J. Comput. Appl. Math.*, **361** (2019), 176–206.

[12] Y. Liu and J. Wang, A locking-free P_0 finite element method for linear elasticity equations on polytopal partitions, preprint, `arXiv:1911.08728`, 2019.

[13] L. Mu, J. Wang, Y. Wang and X. Ye, A weak Galerkin mixed finite element method for biharmonic equations, *Numerical Solution of Partial Differential Equations: Theory, Algorithms, and their Applications*, in: Springer Proceedings in Mathematics and Statistics, **45** (2013), 247–277.

[14] L. Mu, J. Wang, X. Ye and S. Zhang, A C^0-weak Galerkin finite element method for the biharmonic equation, *J. Sci. Comput.*, **59** (2014), 473–495.

[15] P.-A. Raviart and J. M. Thomas, *A Mixed Finite Element Method for Second Order Elliptic Problems*, in: I. Galligani, E. Magenes (Eds.), Mathematical Aspects of the Finite Element

Method, in: Lecture Notes in Math., vol. 606, Springer-Verlag, New York, 1977. Technical Report LA-UR-73-0479, Los Alamos Scientific Laboratory, Los Alamos, NM, 1973.

[16] M. Stynes, Sharp anisotropic interpolation error estimates for rectangular Raviart-Thomas elements, *Math. Comp.*, **83** (2014), 2675-2689.

[17] C. Wang, J. Wang, R. Wang and R. Zhang, A locking-free weak Galerkin finite element method for elasticity problems in the primal formulation, *J. Comput. Appl. Math.*, **307** (2016), 346–366.

[18] R. Wang, X. Wang, Q. Zhai and R. Zhang, A weak Galerkin finite element scheme for solving the stationary Stokes equations, *J. Comput. Appl. Math.*, **302** (2016), 171–185.

[19] J. Wang and X. Ye, A weak Galerkin finite element method for second-order elliptic problems, *J. Comput. Appl. Math.*, **241** (2013), 103–115.

[20] J. Wang and X. Ye, A Weak Galerkin mixed finite element method for second-order elliptic problems, *Math. Comp.*, **83** (2014), 2101–2126.

[21] X. Ye and S. Zhang, A conforming discontinuous Galerkin finite element method, *Int. J. Numer. Anal. and Model.*, **17** (2020), 110–117. arXiv:1904.03331.

[22] X. Ye and S. Zhang, A conforming discontinuous Galerkin finite element method: Part II, arXiv:1907.01397.

[23] H. Zhang, Y. Zou, Y. Xu, Q. Zhai and H. Yue, Weak Galerkin finite element method for second order parabolic equations, *Int. J. Numer. Anal. Model.*, **13** (2016), 525–544.

Received December 2019; 1st revision April 2020; final revision September 2020.

E-mail address: yuefeng19@mails.jlu.edu.cn
E-mail address: liuyj02@pcl.ac.cn
E-mail address: wangrs_math@mail.jlu.edu.cn
E-mail address: szhang@udel.edu